

Detecting and locating volcanic tremors on the Klyuchevskoy group of volcanoes (Kamchatka) based on correlations of continuous seismic records

D.V. Droznin,¹ N.M. Shapiro,^{2,3} S. Ya. Droznina,¹ S.L. Senyukov,¹ V.N. Chebrov¹ and E.I. Gordeev³

¹Kamchatka Branch of the Geophysical Service, Russian Academy of Sciences, 9 Piip Boulevard, Petropavlovsk-Kamchatsky, Kamchatsky Region, Russia

²Institut de Physique du Globe de Paris, Paris Sorbonne Cité, CNRS, 1 rue Jussieu, F-75238 Paris cedex 05, France. E-mail: nshapiro@ipgp.fr

³Institute of Volcanology and Seismology FEB RAS, 9 Piip Boulevard, Petropavlovsk-Kamchatsky, Kamchatsky Region, Russia

Accepted 2015 August 17. Received 2015 July 29; in original form 2015 March 19

SUMMARY

We analyse daily cross-correlation computed from continuous records by permanent stations operating in vicinity of the Klyuchevskoy group of volcanoes (Kamchatka). Seismic waves generated by volcanic tremors are clearly seen on the cross-correlations between some pairs of stations as strong signals at frequencies between 0.2 and 2 Hz and with traveltimes typically shorter than those corresponding to interstation propagation. First, we develop a 2-D source-scanning algorithm based on summation of the envelopes of cross-correlations to detect seismic tremors and to determine locations from which the strong seismic energy is continuously emitted. In an alternative approach, we explore the distinctive character of the cross-correlation waveforms corresponding to tremors emitted by different volcanoes and develop a phase-matching method for detecting volcanic tremors. Application of these methods allows us to detect and to distinguish tremors generated by the Klyuchevskoy and the Tolbachik, volcanoes and to monitor evolution of their intensity in time.

Key words: Time-series analysis; Volcano seismology; Volcano monitoring.

1 INTRODUCTION

Volcanic tremors may be caused by magma moving through narrow cracks, by fragmentation and pulsation of pressurized fluids within the volcano, or by escape of pressurized steam and gases from fumaroles. On many volcanoes, the presence of volcanic tremors is considered as an important attribute of the volcanic unrest and their detection and characterization is used in volcano monitoring systems (e.g. McNutt 1992; Chouet 1996). Volcanic tremors can last from minutes to days and corresponding signals can be very irregular. The simplest method of their characterization is to measure the level of the tremor signal at a single station closely located to the volcano. In areas where separated tremor sources with different locations are acting, more refined algorithms based on records from multiple stations might be necessary for characterizing intensities of the different tremors.

For long period tremors (with frequencies below 0.4 Hz), interstation traveltimes can be accurately measured and used for locating their sources (Haney 2010). At higher frequencies, tremor source locations have been previously determined based on the small aperture arrays (e.g. Goldstein & Chouet 1994; Almendros *et al.* 1997; Métaxian *et al.* 2002) or on the examination of amplitude decay with distance (Battaglia & Aki 2003; Battaglia *et al.* 2005; Taisne *et al.* 2011).

More recently, Ballmer *et al.* (2013) have demonstrated that volcanic tremor can be observed over large distances on interstation cross-correlations of continuous seismic records and that the specific data processing developed for the seismic noise interferometry can be used to locate the tremor sources. Extraction of the Green functions from the noise cross-correlations (e.g. Shapiro & Campillo 2004) used for seismic imaging (e.g. Shapiro *et al.* 2005) or monitoring (e.g. Sens-Schönfelder & Wegler 2006; Wegler & Sens-Schönfelder 2007; Brenguier *et al.* 2008a,b, 2014) relies on a nearly homogeneous distribution of the noise sources. The monitoring can be performed even when the noise distribution is not spatially homogeneous if this distribution does not vary in time resulting in recovery of stable cross-correlation function (e.g. Hadziioannou *et al.* 2009). Such correlation functions recovered from a non-homogeneous noise do not necessary correspond to the media Green function. For example, a strongly localized source continuously emitting seismic waves (such as volcanic tremor) results in appearance of strong ‘spurious’ arrivals whose waveforms and arrival times depend on source location and properties (e.g. Shapiro *et al.* 2006). Therefore, these cross-correlation waveforms can be used to characterize and to locate strong localized seismic sources (e.g. Ballmer *et al.* 2013).

In this paper, we present a study of tremors emitted by the Klyuchevskoy and the Tolbachik volcanoes in Kamchatka. First,

we apply an approach similar to the one suggested by Ballmer *et al.* (2013) to the data recorded between 2009 and 2013 by seismic stations operating in vicinity of the Klyuchevskoy group of volcanoes. We develop a source-scanning algorithm based on summation of the interstation cross-correlation envelopes. This results in the network response function that can be used to detect a tremor and to locate the position of its source. In a next step, we explore the distinctive character of the cross-correlation waveforms corresponding to a particular tremor source to develop a phase-matching detection algorithm.

2 KLYUCHEVSKOY VOLCANIC GROUP

The Klyuchevskoy volcanic group (KVG) is one of largest and most active clusters of subduction-zone volcanoes in the World. The KVG is composed of 13 closely located stratovolcanoes that occupy an area with an average diameter of ~ 70 km (Fig. 1). The 4750 m high Klyuchevskoy Volcano is the most prominent volcano of this cluster with a mean eruptive rate of $1 \text{ m}^3 \text{ s}^{-1}$ over the last 10 kyr (Fedotov *et al.* 1987). It produces lavas of basaltic to basaltic-andesitic composition. Most of the Klyuchevskoy impressive edifice formed within the last 7000 yr according to stratigraphy and ^{14}C radiometric dating (Braitseva *et al.* 1995). The KVG is located in a very particular tectonic setting (Fig. 1), above the edge of the Pacific Plate subducting beneath Kamchatka at the Kamchatka-Aleutian junction. Another important feature is the subduction of the Hawaii–Emperor Seamount (HES) chain. Therefore, geodynamic models proposed to explain the voluminous volcanism in the KVG include the fluid release from the thick, highly hydrated HES crust (e.g. Dorendorf *et al.* 2000), the mantle flow around the corner of the Pacific Plate (e.g. Yogodzinski *et al.* 2001), or the recent detachment of a portion of the subducting slab (e.g. Levin *et al.* 2002; Park *et al.* 2002).

Three volcanoes of the KVG: Klyuchevskoy, Bezymianny and Tolbachik were active during recent decades and produced numerous strong eruptions accompanied by sustained seismic activity (e.g. Ozerov *et al.* 2007; Ivanov 2008; Senyukov *et al.* 2009; Senyukov 2013). The volcano earthquakes together with regional tectonic and teleseismic events were used to study the internal structure of the KVG with the seismic tomography (e.g. Balesta *et al.* 1991; Gorbatoev *et al.* 1999; Slavina *et al.* 2001, 2012; Gontovaia *et al.* 2004; Lees *et al.* 2007; Koulakov *et al.* 2011, 2012) and more recently with an analysis of receiver functions (Nikulin *et al.* 2010; Levin *et al.* 2014).

In this paper, we focus on two recent eruptions of the Klyuchevskoy and the Tolbachik volcanoes (Fig. 1) whose activity is characterized by emission of strong volcanic tremors (e.g. Gordeev *et al.* 1986). The first is the summit eruption of the Klyuchevskoy volcano that continued for about a year in 2009–2010 (e.g. Senyukov 2013). The second one is the fissure eruption of the Tolbachik volcano in 2012–2013 (e.g. Gordeev *et al.* 2013) for which we analyse first 7 months of seismic records.

3 SEISMIC MONITORING NETWORK AND SEISMIC DATA

The Klyuchevskoy group of volcanoes is monitored by seismic network operated by the Kamchatka Branch of the Geophysical Service (KBGS) of the Russian Academy of Sciences (Gordeev *et al.* 2006; Chebrov *et al.* 2013). The positions of 18 seismic stations used in our study are shown in Fig. 1. Stations are three-component

with every component equipped with a CM-3 short period sensor whose corner frequency is approximately 0.8 Hz. The continuous records are tele-transmitted and digitized at 128 samples per second.

4 MONITORING VOLCANIC TREMORS

Main seismic parameters determined by the KBGS for the monitoring of the volcanic activity include the rate and the size of volcanic earthquakes and the level of volcanic tremor. When possible, these seismic parameters are complemented with the visual and the satellite data to determine the level of volcanic alert. The KBGS uses a four-level scale: green–yellow–orange–red. The green colour corresponds to a quiescent state of volcano and the red colour to an ongoing eruption with a plume above 8000 m.

For volcanoes whose eruptions are characterized by emissions of seismic tremors, such as Klyuchevskoy and Tolbachik, the tremor level is one of the key monitored parameters. The tremor monitoring implemented by the KBGS is based on a simple one-station approach. Stations LNG and KMN (Fig. 1) are used to observe the Klyuchevskoy and the Tolbachik tremors, respectively. Examples of 1000 s long vertical component continuous records from these stations are shown in Fig. 2. We show records for 3 d: 05.03.2010, when the Klyuchevskoy volcano was erupting, 28.04.2011, when all volcanoes were quiescent, and 01.12.2012, a few days after the beginning of the Tolbachik eruption. All shown records look like ‘random’ noise and their most distinctive feature is the difference in amplitudes. The RMS amplitudes measured at LNG and KMN are, therefore, used to characterize the Klyuchevskoy and the Tolbachik tremor level, respectively.

The single-station approach described above has at least two obvious limitations. First, the reference stations LNG and KMN are installed in remote areas that are difficult to access. In a case of equipment failure, these stations cannot be immediately repaired and, therefore, they are not operational all the time. The second shortcoming of the one-station amplitude method is that tremors emitted by different sources cannot be easily distinguished. This can be seen in Fig. 2(a) when amplitudes ten times stronger than the quiescent level are recorded on 01.12.2012 by station LNG. This observation can be erroneously interpreted as an increased level of the Klyuchevskoy tremor. In reality, this strong signal was emitted by the erupting Tolbachik volcano. Similarly, the increased signal level at KMN on 05.03.2010 (Fig. 2b) does not correspond to the Tolbachik tremor but results from the Klyuchevskoy activity.

A correct interpretation of the recorded volcanic tremors requires simultaneously analysing signals from several stations. In this paper, we argue that when analysing signals from a network of stations, a more advantageous approach is to use the interstation cross-correlations instead of raw records. These cross-correlations, in addition to the amplitudes, contain information about the relative traveltime delays and about the waveforms. As a consequence, they can be used to characterize sources of seismic tremors more accurately comparing to what can be obtained when using only amplitudes from raw records.

5 CROSS-CORRELATIONS OF CONTINUOUS SEISMIC RECORDS

We followed the approach of Bensen *et al.* (2007) to compute the daily cross-correlations between the vertical-component continuous records of the KVG network. The continuous records were down-sampled from 128 to 8 samples per second and organized in 24-hr

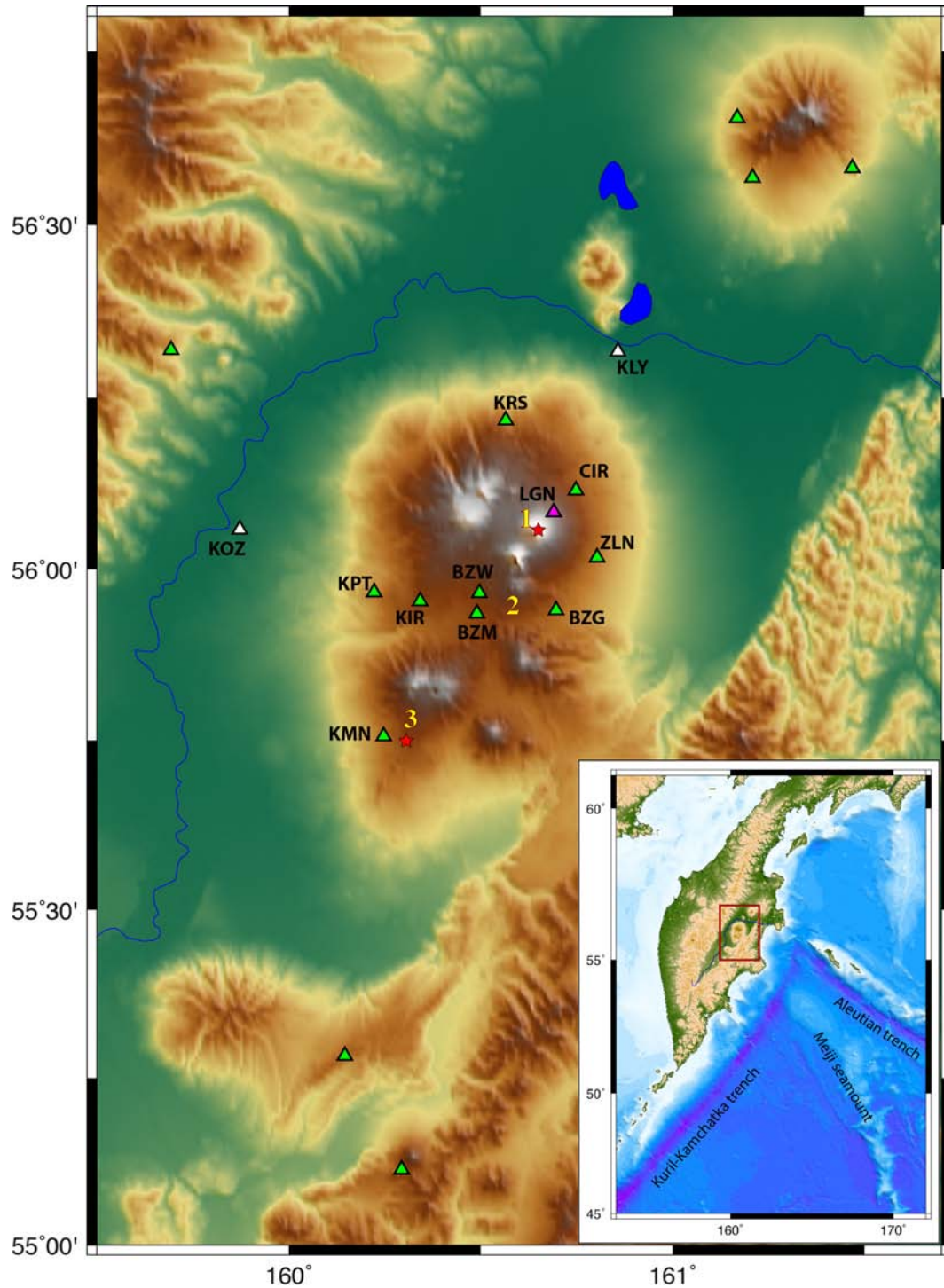


Figure 1. Map of the Klyuchevskoy group of volcanoes with an inset showing the general geographical and tectonic settings. Triangles show position of seismic stations. Names of stations referenced in the paper are indicated. Yellow digits indicate positions of main active volcanoes: (1) Klyuchevskoy, (2) Bezymianny and (3) Tolbachik. Red stars indicate locations of the 2009–2010 Kyuchevskoy and of the 2012–2013 Tolbachik eruptive centres.

long segments. We then applied the spectral whitening between 0.1 and 4 Hz followed by the one-bit normalization. Then, daily cross-correlations for 153 stations pairs were computed during the period between 01.01.2009 and 07.07.2013.

Examples of cross-correlations are shown in Fig. 3. First, we note that Rayleigh wave parts of Green functions are not clearly emerging from the noise even if year-long cross-correlations are stacked (Fig. 3a). The reason for such behaviour is that the recorded

wavefield is often dominated by volcanic tremors whose sources are strongly localized in space and not by the ambient noise with well-distributed sources. This can be clearly seen from the visual inspection of day-long cross-correlations (for dates illustrated in Fig. 2). Fig. 3(b) show cross-correlations computed during 1 d when all surrounding volcanoes were quiet and in this case no clear signals emerge after correlating just 1 d of the noise. Fig. 3(c) shows a day-long cross-correlation computed during a period of strong

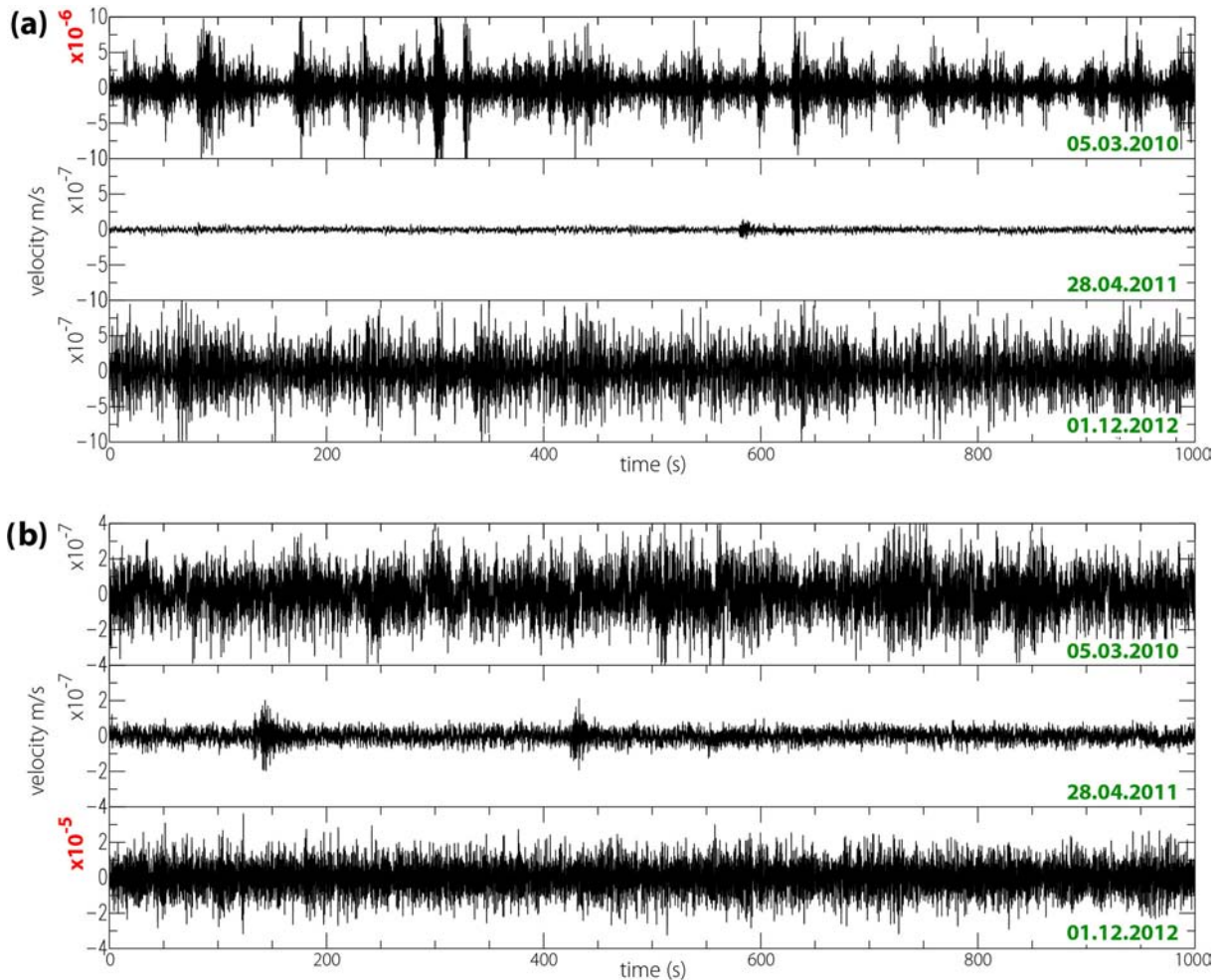


Figure 2. Examples of continuous records from stations LGN (a) and KMN (b) (see Fig. 1 for station locations). Corresponding dates are indicated with green numbers. Note the differences in the vertical scales as indicated with red numbers.

activity of the Klyuchevskoy volcano. In this case, strong one-sided signals emerge in all cross-correlations. A close inspection show that this signal propagates from a vicinity of station LGN (closest station to the active crater of the Klyuchevskoy volcano) to all other stations. If we consider another day, when the Tobachik volcano was active (Fig. 3d), we see again strong emerging asymmetric signals. However, their shapes and relative traveltimes are very different from those recorded during the period of the Klyuchevskoy activity.

6 SOURCE-SCANNING ALGORITHM FOR DETECTION AND LOCATION OF TREMORS

Waveforms shown in Figs 3(c) and (d) clearly show that correlations of continuous seismic records recorded in vicinity of volcanoes during the periods of their activity can be dominated by seismic tremors emitted by these volcanoes. This implies, in turn, that the cross-correlations can be used to detect and locate the sources of these tremors.

We first explore the approach similar to the one described by Ballmer *et al.* (2013) and develop a method that we call the source-scanning algorithm. The idea is to consider that tremors are emitted by sources localized in space and to use the differential traveltimes of signals appearing in interstation cross-correlations to characterize

the locations of tremor sources. The method consists of following steps.

- (1) We compute smoothed envelopes from cross-correlation waveforms.
- (2) We compute traveltimes for all stations for every tested source position.
- (3) We shift the smoothed envelopes based on differential interstation traveltimes.
- (4) We compute the sum of the shifted envelopes at zero time.

The resulting function called the network response characterizes the likelihood of location of a seismic source in a particular position.

We compute cross-correlations between stations i and j : $C^{i,j}(t)$ and use the following recursive averaging algorithm to compute their smoothed envelopes $S^{i,j}(t)$:

$$S_k^{i,j} = S_{k-1}^{i,j} + \left(\left| C_k^{i,j} \right| - S_{k-1}^{i,j} \right) / M, \quad (1)$$

where index k indicates the time sample and M is the averaging coefficient expressed in number of time steps. We empirically selected the value of $M = 240$ that approximately corresponds to a 30 s averaging window. The eq. (1) is applied twice in two directions to compensate for a possible time-shift. This smoothing is necessary to compensate for uncertainties in the predicted traveltimes used to shift the waveforms, as described in the following paragraph.

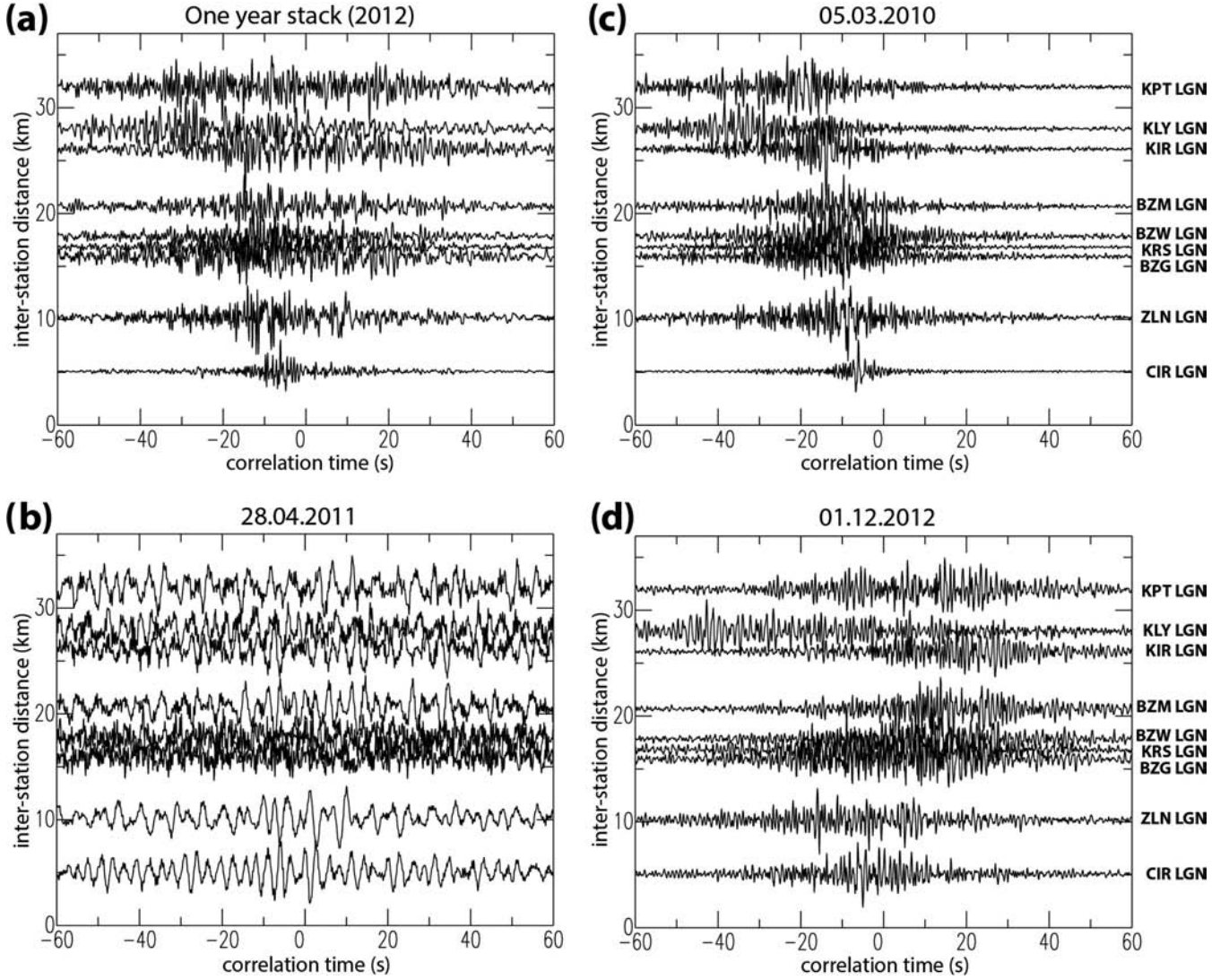


Figure 3. Example of cross-correlations of vertical component records between stations LGN shown with a magenta triangle in Fig. 1 and a set of other stations. (a) Cross-correlations stacked over 2012. (b–d) Day-long cross-correlations computed for dates illustrated in Fig. 2.

Traveltimes $t^i(r)$ are estimated as function of distance $d^i(r)$ between the tested source position r and the station i based on average traveltimes curve estimated for the KVG regions explained in the Appendix. The final network response function is computed as a sum of shifted smoothed envelopes:

$$R(r) = \sum_{i=1}^N \sum_{j=i+1}^N S^{i,j} [t^i(r) - t^j(r)], \quad (2)$$

where N is the total number of used stations. We consider that sources of seismic tremors are located very close to the surface and compute values of $R(r)$ on a 2-D geographical grid within a region shown in Fig. 3. The size of the grid elements is 0.02 in latitude and 0.04 in longitude. For visualization, we renormalize the network response:

$$\tilde{R}(r) = \frac{R(r) - R^{\min}}{R^{\max} - R^{\min}}, \quad (3)$$

where R^{\max} and R^{\min} are the absolute maximum and minimum of $R(r)$. To compare network responses computed during different days, we estimate their normalized maxima:

$$\tilde{R}^{\max}(n^d) = 100 \times \frac{R^{\max}(n^d) - R^{\min}(n^d)}{R^{\text{ref}}}, \quad (4)$$

where n^d is the day number or date and R^{ref} is a normalization coefficient. We arbitrary selected R^{ref} as an average of $R^{\max} - R^{\min}$ over March 2010, a period of strong activity of the Klyuchevskoy volcano.

Results of computation of \tilde{R}^{\max} from 18 used stations (153 interstation cross-correlations) for the whole period of study (01.01.2009–07.07.2013) and examples of $\tilde{R}(r)$ for 3 d are shown in Fig. 4. It can be seen that the values of \tilde{R}^{\max} are very high during eruptions of Klyuchevskoy (Fig. 4a) and Tolbachik (Fig. 4c) and becomes very low during the period of volcanic quiescence (Fig. 4b). During the eruptive periods, the maps of $\tilde{R}(r)$ exhibit strong and clear maxima in vicinity of the eruptive centres (Figs 4a and c). We note that the weak maximum during the ‘quiet’ day (28.04.2011) is also located in vicinity of volcanoes (Fig. 4b) possibly indicating some minor activity.

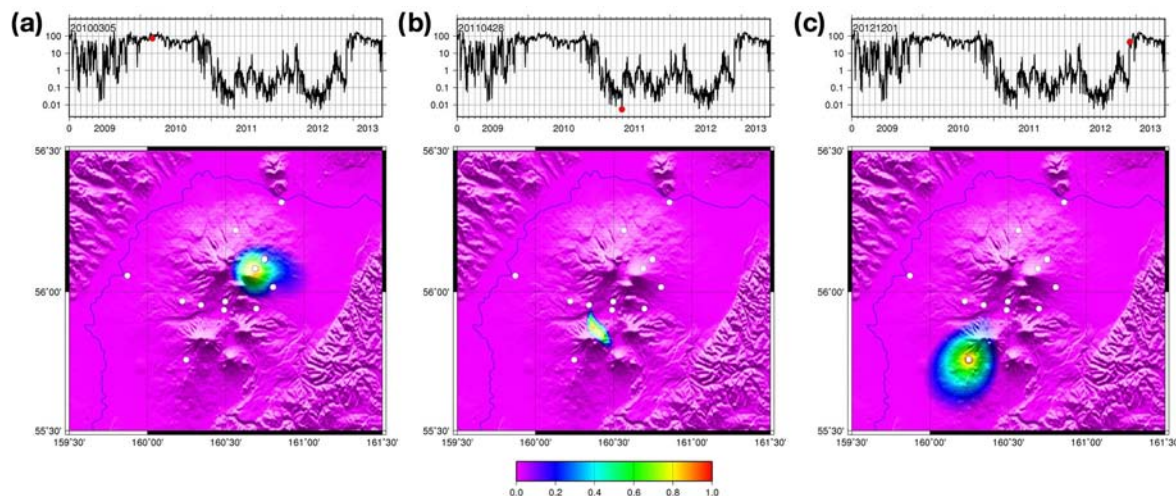


Figure 4. Network response functions \tilde{R}^{\max} (eq. 4) and $\tilde{R}(r)$ (eq. 3) for dates illustrated in Figs 2 and 3 shown in upper and lower frames, respectively. (a) A day during the Klyuchevskoy eruption. (b) A day without volcanic activity. (c) A day during the Tolbachik eruption. Corresponding dates are indicated in upper frames with text and red circles. White circles in lower frames show station positions.

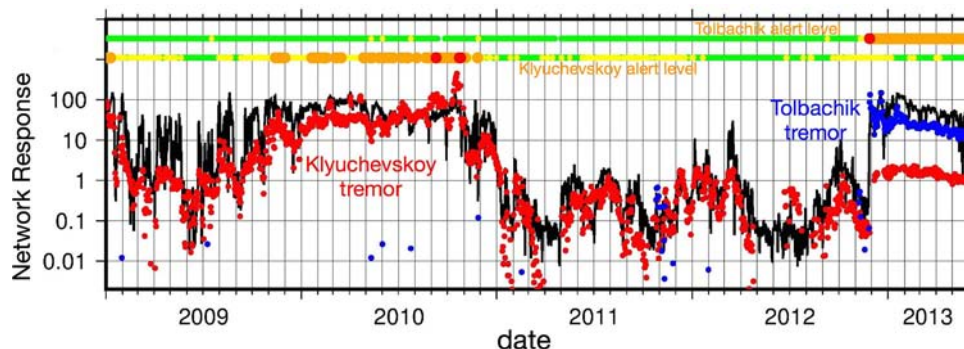


Figure 5. Comparison of the network response function \tilde{R}^{\max} (eq. 4) shown with the solid black line with normalized tremor amplitudes for Klyuchevskoy and Tolbachik volcanoes shown with red and blue dots, respectively. Colour circles in the upper part of the figure show alert levels (see description in Section 4) for Klyuchevskoy (below) and Tolbachik (above) volcanoes.

In Fig. 5, we compare values of \tilde{R}^{\max} with daily average levels of tremors routinely determined by the KBGS operators. As explained in Section 4, for the Klyuchevskoy volcano, they use as reference station LGN and for Tolbachik KMN. During the Tolbachik eruption, the emitted tremor was so strong that it was also recorded at stations LGN and interpreted as a moderate-level tremor of Klyuchevskoy (Fig. 5). This example shows that single-stations measurements cannot always distinguish unambiguously the origin of seismic tremor. The temporal variations of \tilde{R}^{\max} follow very closely the tremor levels determined by operators. We note that the network response used in our study is based on cross-correlations computed from binarized seismograms (following Bensen *et al.* 2007) and therefore is not affected by the amplitudes of the recorded wavefield but only by its level of coherency. Overall, the results presented in Figs 4 and 5 clearly demonstrate that the network response expressed in form of functions $\tilde{R}(r)$ (eq. 3) and \tilde{R}^{\max} (eq. 4) is very sensitive to the level of volcanic tremors and can be used to distinguish their origin from different volcanoes.

7 DETECTING TREMORS WITH A PHASE-MATCHING APPROACH

Because of the irregular temporal behaviour of the tremor source, corresponding seismic records look like random signals (Fig. 2).

Despite this, if the position of the tremor source remains in the same location, seismic waves propagating between the tremor source and a particular station follow the same path and contain a fixed imprint of the media. After computing a cross-correlation between a pair of stations, the irregular source time function is cancelled and the resulting waveform represents a sort of ‘interference’ of two propagation patterns and remains stable in time.

The scenario described above can be realized when an eruptive centre of a volcano remains in the same position during long eruptive episodes. In this case, the cross-correlation waveforms computed from different time windows during these episodes will remain stable in time. This property is illustrated in Fig. 6(a) that shows cross-correlations computed between CIR and LGN during 8 consecutive days in January 2010 when the Klyuchevskoy volcano erupted.

When the location of the tremor source is changed and the propagation of seismic waves between this source and the considered stations becomes very different. As a consequence, the shape of the correlation waveforms computed between the same pair of station becomes very different as illustrated in Fig. 6(c) showing cross-correlations computed between CIR and LGN during 8 consecutive days in January 2013 when the Tolbachik volcano erupted.

The presented examples show that cross-correlations computed between a single station pair are very sensitive to the location of

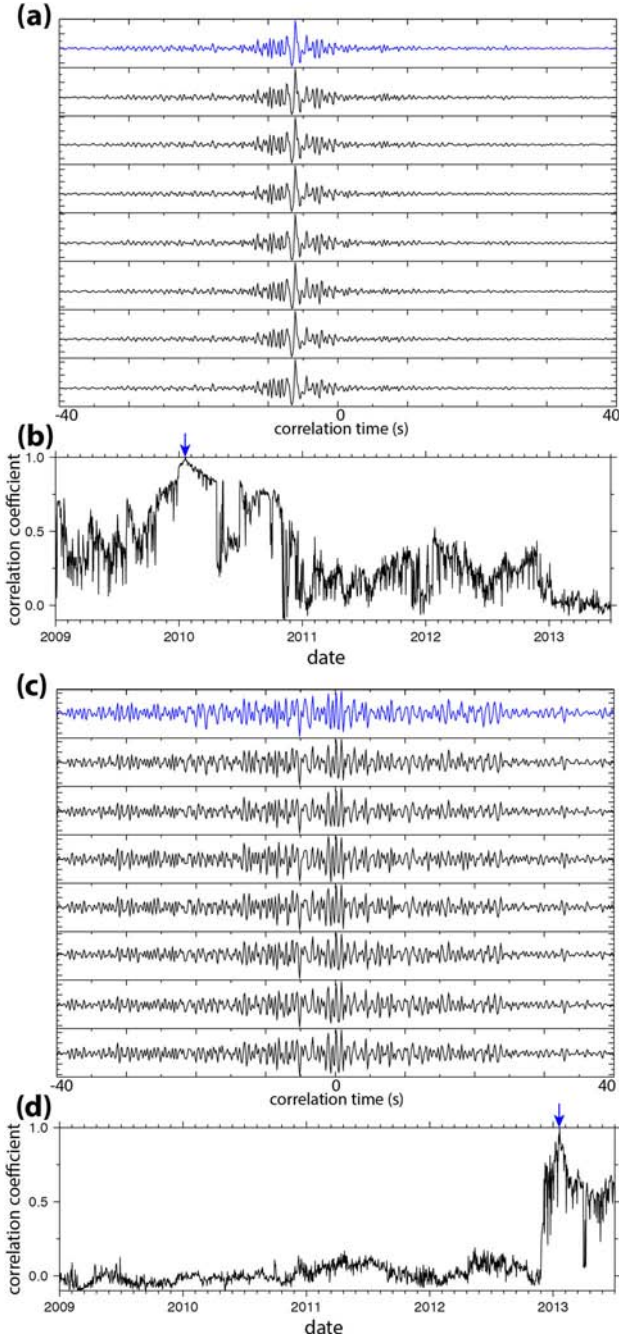


Figure 6. Analysis of similarity of daily cross-correlations between stations CIR and LGN. (a) Daily cross-correlations during the Klyuchevskoy eruption: between 2010 January 20 and January 27. (b) Correlation coefficient between all daily cross-correlations and the reference waveforms corresponding to the Klyuchevskoy eruption (the correlation for 2010 January 20 show with the blue colour in (a) and indicated with the blue arrow). (c) Daily cross-correlations during the Tolbachik eruption: between 2013 January 20 and 27. (d) Correlation coefficient between all daily cross-correlations and the reference waveforms corresponding to the Tolbachik eruption (the correlation for January 20, 2013 shown with the blue colour in (c) and indicated with the blue arrow).

the source of volcanic tremor and can be used as a ‘fingerprint’ characteristic for the activity of a particular volcano. To explore this idea, we selected the daily cross-correlation between CIR and LGN for 2010 January 20 as a reference and estimated its similarity with all daily cross-correlations computed between the same pair

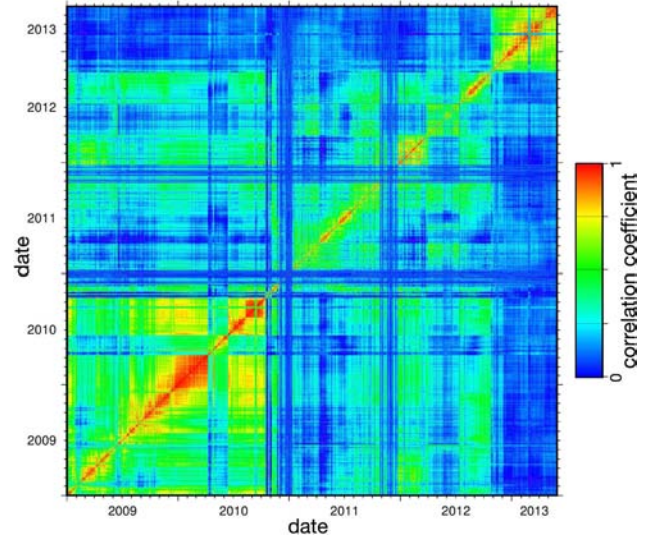


Figure 7. Matrix of correlation coefficients between all daily cross-correlation waveforms for the station pair CIR-LGN.

of stations during the whole period of study. We used a simple correlation coefficient $C_{\text{coeff}}^{\text{KM}}$ between cross-correlation waveforms for dates K and M as a measure of their similarity:

$$C_{\text{coeff}}^{\text{KM}} = \frac{\sum_{i=-n}^n cc_i^K cc_i^M}{\sqrt{\sum_{i=-n}^n cc_i^K cc_i^K \sum_{i=-n}^n cc_i^M cc_i^M}}, \quad (5)$$

where cc_i^K and cc_i^M are samples of respective cross-correlations at time t_i . We use a time window between -50 and 50 s. With the sampling rate of 8 samples per second, this leads to $n = 400$ in eq. (5). The results of this computation shown in Fig. 6(b) delineate well main periods of the Klyuchevskoy activity (as can be seen in comparison with Fig. 5) while during the Tolbachik eruption the values of the correlation coefficient remain very low. When we use as reference the daily cross-correlation for 2013 January 20 the resulting curve (Fig. 6d) delineates very clearly the Tolbachik eruption.

The reference waveforms used for the ‘phase-matched’ detection of tremors shown in Fig. 6 were selected arbitrary. With this approach, the efficiency of the detection could be deteriorated if the selected ‘reference’ date was not representative for the most typical tremors. Fig. 7 shows a matrix of correlation coefficients computed between all daily cross-correlations during the period of study. This matrix is symmetric and its rows (or columns) are equivalent to curves shown in Figs 6(b) and (d) with using different daily cross-correlation waveforms as references.

A more robust approach for selection of reference waveforms for the phase-matched detection is based on extraction of cross-correlations that are most representative for the considered period of time. For this goal we use the principal component analysis (PCA; e.g. Murtagh & Heck 1987) of the ensemble of daily cross-correlations. We compute a matrix of sums of cross products between all available cross-correlation waveforms:

$$C_{lk} = \sum_{i=1}^{N_{\text{dates}}} cc_i^l cc_i^k, \quad l, k = 1, N_{\text{samples}}, \quad (6)$$

where cc_i^l and cc_i^k are samples of cross-correlations for the date i at times t_l and t_k . N_{dates} and N_{samples} are numbers of available dates and

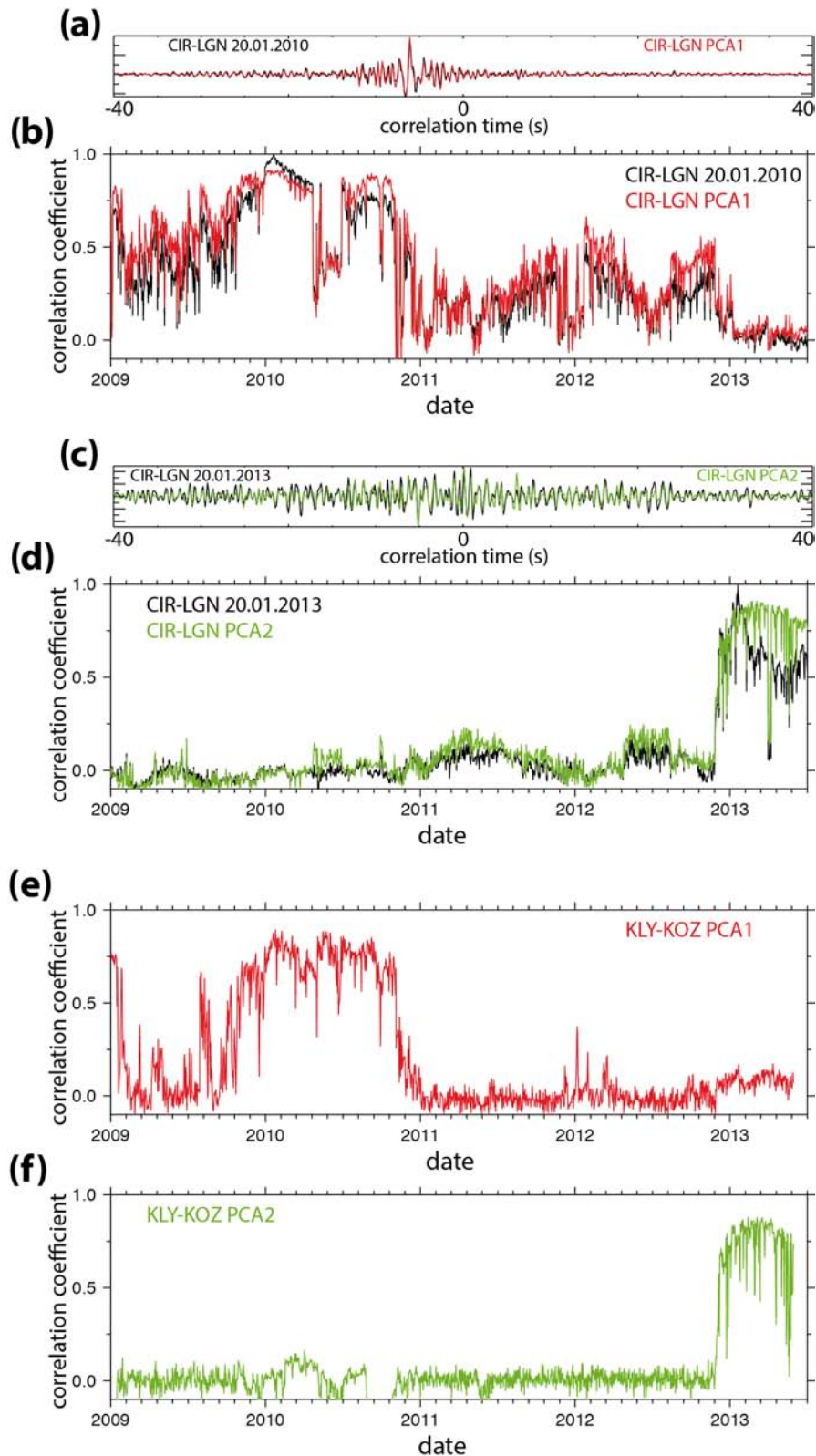


Figure 8. Result of the phase-matched tremor detection based on waveforms determined with the principal component analysis (PCA). (a) and (c) Waveforms corresponding to the first and the second maximum singular values, respectively, of the PCA of the ensemble of daily cross-correlations between stations CIR and LGN. Daily cross-correlations for 20.01.2010 and 20.01.2013 are shown with black lines, for reference. (b) and (d) Correlation coefficients between all daily cross-correlations and the waveforms corresponding to the first and the second PCA maximum singular values for the station pair CIR-LGN. Result from Figs 6(c) and (d) are shown with black lines, for reference. (e) and (f) Correlation coefficients between all daily cross-correlations and the waveforms corresponding to the first and the second PCA maximum singular values for the station pair KLY-KOZ (shown with white triangles in Fig. 1).

on of samples in every waveform, respectively (in the case of pair CIR-LGN, we use $N_{\text{dates}} = 1644$ and $N_{\text{samples}} = 801$). Eq. (6) results in a square matrix with the dimension of N_{samples} . The PCA consists in computing its eigenvalues and corresponding eigenvectors that are called principal components. The principal components corresponding to maximal eigenvalues are representative of common features contained in the ensemble of analysed waveforms.

Waveforms corresponding for two first principal components for the station pair CIR-LGN are shown in Figs 8(a) and (c). They are remarkably similar to the daily cross-correlations computed during typical periods of activity of the Klyuchevskoy and the Tolbachik volcanoes, respectively. The phase-matched detections based on these PCA extracted waveforms are shown with red and green lines in Figs 8(b) and (d), respectively.

We then apply the PCA to the 1587 daily cross-correlations available for the pair KLY-KOZ. These two stations (shown with white triangles in Fig. 1) are located relatively far from the volcanoes comparing to stations CIR and LGN. The phase-matched detections based on waveforms corresponding to two maximum PCA eigenvalues presented in Figs 8(e) and (f) show that, similarly to the results from CIR-LGN, the Klyuchevskoy and the Tolbachik eruptions are clearly detected.

8 DISCUSSION AND CONCLUSION

We analysed cross-correlations of continuous records by seismic stations located in vicinity of the Klyuchevskoy group of volcanoes. During periods of strong volcanic activity these cross-correlations do not converge to interstations Green functions and are dominated by arrivals from well-localized sources of volcanic tremors. This observation first indicates that certain precautions are required when applying the monitoring methods based on correlations of seismic noise to active volcanoes. In a case of volcanoes generating strong seismic tremors, the correlations waveforms and their variations in time can be significantly affected by these tremors. These source-caused time variations could be mistaken with possible structural changes.

The tremor-generated signals in the cross-correlations can, in turn, be used for monitoring the tremor activity that is one of the important features of the volcanic unrest. We first develop and apply a source-scanning algorithm based on analysis of cross-correlations computed for the whole network similar to the approach developed by Ballmer *et al.* (2013). The network response function $\tilde{R}(r)$ can be used to find the geographical location of the tremor source and variation of its maximum \tilde{R}^{max} in time is a good proxy to the tremor intensity. Another promising approach is to use the characteristic shape of cross-correlations computed during periods of strong tremors as a ‘fingerprint’ of this tremor activity. We have shown that this approach applied to just one pair of stations results in a very efficient phase-matched detection of tremors generated by different volcanoes.

ACKNOWLEDGEMENTS

All seismological observations used in this study were provided by the Kamchatkan Branch of Geophysical Survey of Russian Academy of Sciences (<http://www.emsd.ru>). This research was supported by the Russian Science Foundation (grant 14-47-00002) as well as by the French projects ‘Labex UnivEarth’ and by the Université Sorbonne Paris Cité via project ‘VolcanoDynamics’.

REFERENCES

- Almendros, J., Ibanez, J.M., Alguacil, G., Del Pezzo, E. & Ortiz, R., 1997. Array tracking of the volcanic tremor source at Deception Island, Antarctica, *Geophys. Res. Lett.*, **24**(23), 3069–3072.
- Balesta, S.T., Gontovaia, L.I., Kargopoltsev, V.A., Pak, G., Pushkarev, V.G. & Senyukov, S.L., 1991. Results of seismic investigations of the crust in the region of the Klyuchevskoy, volcano, *Volcanol. Seismol.*, **3**, 3–18.
- Ballmer, S., Wolfe, C.J., Okubo, P.G., Haney, M.M. & Thurber, C.H., 2013. Ambient seismic noise interferometry in Hawai’i reveals long-range observability of volcanic tremor, *Geophys. J. Int.*, **194**, 512–523.
- Battaglia, J. & Aki, K., 2003. Location of seismic events and eruptive fissures on the Piton de la Fournaise volcano using seismic amplitudes, *J. geophys. Res.*, **108**(B8), 2364, doi:10.1029/2002JB002193.
- Battaglia, J., Aki, K. & Ferrazzini, V., 2005. Location of tremor sources and estimation of lava output using tremor source amplitude on the Piton de la Fournaise volcano: 1. Location of tremor sources, *J. Volc. Geotherm. Res.*, **147**, 268–290.
- Bensen, G.D., Ritzwoller, M.H., Barmin, M.P., Levshin, A.L., Lin, F.C., Moschetti, M.P., Shapiro, N.M. & Yang, Y., 2007. Processing seismic ambient noise data to obtain reliable broad-band surface wave dispersion measurements, *Geophys. J. Int.*, **169**, 1239–1260.
- Braitseva, O.A., Melekestsev, I.V., Ponomareva, V.V. & Sulerzhitsky, L.D., 1995. The ages of calderas, large explosive craters and active volcanoes in the Kuril–Kamchatka region, *Bull. Volcanol.*, **57**, 383–402.
- Brenguier, F., Shapiro, N.M., Campillo, M., Ferrazzini, V., Duputel, Z., Coutant, O. & Necessian, A., 2008a. Towards forecasting volcanic eruptions using seismic noise, *Nat. Geosci.*, **1**, 126–130.
- Brenguier, F., Campillo, M., Hadziioannou, C., Shapiro, N.M., R.M. Nadeau, R.M. & Larose, E., 2008b. Postseismic relaxation along the San Andreas Fault at Parkfield from continuous seismological observations, *Science*, **321**, 1478–1481.
- Brenguier, F., Campillo, M., Takeda, T., Aoki, Y., Shapiro, N.M., Briand, X., Emoto, K. & Miyake, H., 2014. Mapping pressurized volcanic fluids from induced crustal seismic velocity drops, *Science*, **345**(6192), 80–82.
- Chebrov, V.N., Droznin, D.V., Kugaenko, Y.A., Levina, V.I., Senyukov, S.L., Sergeev, V.A., Shevchenko, Y.V. & Yashchuk, V.V., 2013. The system of detailed seismological observations in Kamchatka in 2011, *J. Volc. Seismol.*, **5**(3), 161–170.
- Chouet, B.A., 1996. Long-period volcano seismicity: its source and use in eruption forecasting, *Nature*, **380**, 309–316.
- Dorendorf, F., Wiechert, U. & Wörner, G., 2000. Hydrated sub-arc mantle: a source for the Klyuchevskoy volcano, Kamchatka/Russia, *Earth planet. Sci. Lett.*, **175**, 69–86.
- Fedotov, S.A., Khrenov, A.P. & Jarinov, N.A., 1987. Klyuchevskoy volcano, its activity in 1932–1986 and possible development, *Volcanol. Seismol.*, **4**, 3–16.
- Goldstein, P. & Chouet, B., 1994. Array measurements and modeling of sources of shallow volcanic tremor at Kilauea volcano, Hawaii, *J. geophys. Res.*, **99**(B2), 2637–2652.
- Gontovaia, L.I., Khrenov, A.P., Stepanova, M.Y. & Senyukov, S.L., 2004. Model of the deep lithosphere in the region of the Klyuchevskoy group of volcanoes, *Volcanol. Seismol.*, **3**, 3–11.
- Gorbatov, A., Domínguez, J., Suárez, G., Kostoglodov, V., Zhao, D. & Gordeev, E.I., 1999. Tomographic imaging of the P-wave velocity structure beneath the Kamchatka peninsula, *Geophys. J. Int.*, **137**, 269–279.
- Gordeev, E.I., Melnikov, Y.Y., Sinitsin, V.I. & Chebrov, V.N., 1986. Volcanic tremor of the Klyuchevskoy volcano (summit eruption in 1984), *Volcanol. Seismol.*, **5**, 39–53.
- Gordeev, E.I., Chebrov, V.N., Levina, V.I., Senyukov, S.L., Shevchenko, Y.V. & Yashuk, V.V., 2006. System of seismological observations in Kamchatka, *Volcanol. Seismol.*, **3**, 6–27.
- Gordeev, E.I., Muravyev, Y.D., Samoylenko, S.B., Volynets, A.O., Melnikov, D.V. & Dvigalo, V.N., 2013. The Tolbachik fissure eruption of 2012–2013: preliminary results, *Doklady Earth Sci.*, **452**(2), 1046–1050.
- Hadziioannou, C., Larose, E., Coutant, O., Roux, P. & Campillo, M., 2009. Stability of monitoring weak changes in multiply scattering media with

- ambient noise correlation: laboratory experiments, *J. acoust. Soc. Am.*, **125**(6), 3688–3695.
- Haney, M.M., 2010. Location and mechanism of very long period tremor during the 2008 eruption of Okmok Volcano from interstation arrival times, *J. geophys. Res.*, **115**, B00B05, doi:10.1029/2010JB007440.
- Ivanov, V.V., 2008. Current cycle of the Kluchevskoy volcano activity in 1995–2008 based on seismological, photo, video and visual data, in *Proceedings of Sci. Conf. Devoted to Volcanologist Day. 2008 March 27–29 March 2008, Petropavlovsk-Kamchatsky: IVS RAS, Petropavlovsk-Kamchatsky, 27–29 March*, pp. 100–109.
- Koulakov, I., Gordeev, E.I., Dobretsov, N.L., Vernikovskiy, V.A., Senyukov, S.L. & Jakovlev, A., 2011. Feeding volcanoes of the Kluchevskoy group from the results of local earthquake tomography, *Geophys. Res. Lett.*, **38**, L09305, doi:10.1029/2011GL046957.
- Koulakov, I., Gordeev, E.I., Dobretsov, N.L., Vernikovskiy, V.A., Senyukov, S.L., Jakovlev, A. & Jaxybulatov, K., 2012. Rapid changes in magma storage beneath the Klyuchevskoy group of volcanoes inferred from time-dependent seismic tomography, *J. Volc. Geotherm. Res.*, **263**, 75–91.
- Lees, J.M., Symons, N., Chubarova, O., Gorelchik, V. & Ozerov, A., 2007. Tomographic images of Kluchevskoi volcano P-wave Velocity, in *Volcanism and Subduction: The Kamchatka Region*, pp. 293–302, eds Eichelberger, J., Gordeev, E., Kasahara, M., Izbekov, P. & Lees, J.M., American Geophysical Union.
- Levin, V., Shapiro, N.M., Park, J. & Ritzwoller, M.H., 2002. Seismic evidence for catastrophic slab loss beneath Kamchatka, *Nature*, **418**, 763–767.
- Levin, V., Droznina, S., Gavrilenko, M., Carr, M. & Senyukov, S., 2014. Seismically active sub-crustal magma source of the Klyuchevskoy volcano in Kamchatka, Russia, *Geology*, **42**(11), 983–986.
- McNutt, S.R., 1992. Volcanic Tremor, in *Encyclopedia of Earth System Science*, pp. 417–425, Academic Press.
- Métaxian, J.-P., Lesage, P. & Valette, B., 2002. Locating sources of volcanic tremor and emergent events by seismic triangulation: application to Arenal volcano, Costa Rica, *J. geophys. Res.*, **107**(B10), 2243, doi:10.1029/2001JB000559.
- Murtagh, F. & Heck, A., 1987. *Multivariate Data Analysis*, Kluwer Academic.
- Nikulin, A., Levin, V., Shuler, A. & West, M., 2010. Anomalous seismic structure beneath the Klyuchevskoy Group, Kamchatka, *Geophys. Res. Lett.*, **37**, L14311, doi:10.1029/2010GL043904.
- Ozerov, A.Y., Firstov, P.P. & Gavrilov, V.A., 2007. Periodicities in the dynamics of eruptions of Klyuchevskoi Volcano, Kamchatka, *Volc. Subduct.: Kamchatka Region: Geophys. Monogr. Ser.*, **172**, 283–291.
- Park, J., Levin, V., Brandon, M.T., Lees, J.M., Peyton, V., Gordeev, E. & Ozerov, A., 2002. A dangling slab, amplified arc volcanism, mantle flow and seismic anisotropy near the Kamchatka plate corner, in *Plate Boundary Zones*, pp. 295–324, eds Seth, S. & Jeffrey, F., AGU Geodynamics Series No. 30, AGU.
- Sens-Schönfelder, C. & Wegler, U., 2006. Passive image interferometry and seasonal variations of seismic velocities at Merapi Volcano, Indonesia, *Geophys. Res. Lett.*, **33**, L21302, doi:10.1029/2006GL027797.
- Senyukov, S.L., 2013. Monitoring and forecasting of the activity of the Kamchatka volcanoes based on seismological data during 2000–2010, *Volcanol. Seismol.*, **1**, 96–108.
- Senyukov, S.L., Droznina, S.Ya., Nuzhdina, I.N., Garbuzova, V.T. & Kozhenkova, T.Y., 2009. Studies in the activity of Klyuchevskoi volcano by remote sensing techniques between January 1, 2001 and July 31, 2005, *Volcanol. Seismol.*, **3**, 50–59.
- Shapiro, N.M. & Campillo, M., 2004. Emergence of broadband Rayleigh waves from correlations of the ambient seismic noise, *Geophys. Res. Lett.*, **31**, L07614, doi:10.1029/2004GL019491.
- Shapiro, N.M., Campillo, M., Stehly, L. & Ritzwoller, M.H., 2005. High resolution surface wave tomography from ambient seismic noise, *Science*, **307**, 1615–1618.
- Shapiro, N.M., Ritzwoller, M.H. & Bensen, G.D., 2006. Source location of the 26 sec microseism from cross-correlations of ambient seismic noise, *Geophys. Res. Lett.*, **33**, L18310, doi:10.1029/2006GL027010.

- Slavina, L.B., Garagi, I.A., Gorelchik, V.I., Ivanov, B.V. & Belyankin, B.A., 2001. Velocity structure and stress-deformation state of the crust in the area of the Kluchevskoy volcano group in Kamchatka, *Volcanol. Seismol.*, **1**, 49–59.
- Slavina, L.B., Pivovarova, N.B. & Senyukov, S.L., 2012. Dynamics of the seismic structure of the northern group of volcanoes in Kamchatka and its relation with the volcanic activity, *Volcanol. Seismol.*, **2**, 39–55.
- Taisne, B., Brenguier, F., Shapiro, N.M. & Ferrazzini, V., 2011. Imaging the dynamics of magma propagation using radiated seismic intensity, *Geophys. Res. Lett.*, **38**, L04304, doi:10.1029/2010GL046068.
- Wegler, U. & Sens-Schönfelder, C., 2007. Fault zone monitoring with passive image interferometry, *Geophys. J. Int.*, **168**, 1029–1033.
- Yogodzinski, G.M., Lees, J.M., Churikova, T.G., Dorendorf, F., Woerner, G. & Volynets, O.N., 2001. Geochemical evidence for the melting of subducting oceanic lithosphere at plate edges, *Nature*, **409**, 500–504.

APPENDIX

We stacked cross-correlations during the time of the Klyuchevskoy eruption (01.01.2010–30.09.2010). During this period, we can reasonably assume that the source of seismic tremor is located within the crater of the Klyuchevskoy volcano. Therefore, we selected the closest stations to this crater LGN as reference and considered cross-correlations between this station and all others. We then measured delay times t corresponding to arrivals of maximum energy and compared with differential distances d computed as difference between distances from stations to the Klyuchevskoy crater (tremor source). The resulting measurements are shown in Fig. A1 with black squares. A reasonable fit to this ensemble of delay times is found with a simple power-law equation:

$$t = 2.36 d^{0.68}, \quad (\text{A1})$$

where time delays are in seconds and distances are in kilometres. The resulting traveltime curve shown with the red line in Fig. A1 is used in estimation of the network response function with eq. (2).

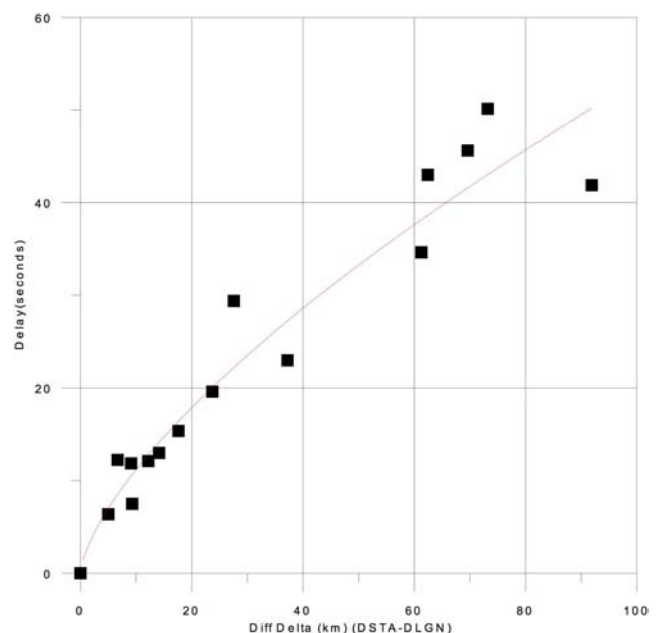


Figure A1. Interstations delay times as function of distance difference to the Klyuchevskoy crater. Station LGN is used as reference. Black squares show observations. The best-fitting traveltime curve is shown with the red curve.